Effects of Three-Nucleon Forces and Two-Body Currents on Gamow-Teller Strengths

A. Ekström,[1] G. R. Jansen,[2,3] K. A. Wendt,[3,2] G. Hagen,[2,3] T. Papenbrock,[3,2] S. Bacca,[4,5] B. Carlsson,[6] and D. Gazit[7]
[1]Department of Physics and Center of Mathematics for Applications, University of Oslo, N-0316 Oslo, Norway
[2]Physics Division, Oak Ridge National Laboratory, Oak Ridge, Tennessee 37831, USA
[3]Department of Physics and Astronomy, University of Tennessee, Knoxville, Tennessee 37996, USA
[4]TRIUMF, 4004 Wesbrook Mall, Vancouver, British Columbia V6T 2A3, Canada
[5]Department of Physics and Astronomy, University of Manitoba, Winnipeg, Manitoba R3T 2N2, Canada
[6]Department of Fundamental Physics, Chalmers University of Technology, SE-412 96 Göteborg, Sweden
[7]Racah Institute of Physics, Hebrew University, 91904 Jerusalem, Israel
(Received 18 June 2014; revised manuscript received 7 November 2014; published 30 December 2014)

We optimize chiral interactions at next-to-next-to leading order to observables in two- and three-nucleon systems and compute Gamow-Teller transitions in ^{14}C and ^{22,24}O using consistent two-body currents. We compute spectra of the daughter nuclei ^{14}N and ^{22,24}F via an isospin-breaking coupled-cluster technique, with several predictions. The two-body currents reduce the Ikeda sum rule, corresponding to a quenching factor $q^2 \approx 0.84$–0.92 of the axial-vector coupling. The half-life of ^{14}C depends on the energy of the first excited 1^+ state, the three-nucleon force, and the two-body current.

DOI: 10.1103/PhysRevLett.113.262504 PACS numbers: 23.40.-s, 21.10.-k, 21.30.-x, 24.10.Cn

Introduction.—β decay is one of the most interesting processes and most useful tools in nuclear physics. On the one hand, searches for neutrinoless double-β decay probe physics beyond the standard model and basic properties of the neutrino; see Avignone *et al.* [1] for a recent review. If neutrinoless double-β decay is observed, an accurate nuclear-physics matrix element is needed to extract neutrino masses from the lifetime. On the other hand, β decay of rare isotopes populates states in exotic nuclei and thereby serves as a spectroscopic tool [2,3]. The theoretical calculation of electroweak transition matrix elements in atomic nuclei is a challenging task because it requires an accurate description of the structure of the mother and daughter nuclei and an employment of a transition operator that is consistent with the Hamiltonian.

For the transition operator, the focus is on the role of two-body currents (2BCs) from chiral effective field theory (χEFT) [4]. Two-body currents are related to three-nucleon forces (3NFs) [5,6] because the low energy constants (LECs) of the latter constrain the former within χEFT. Consistency of Hamiltonians and currents is one of the hallmarks of an EFT [7], and 2BCs are applied in electromagnetic processes of light nuclei; see Kölling *et al.* [8], Grießhammer *et al.* [9], and Pastore *et al.* [10], and see Bacca and Pastore [11] for a recent review. For weak decays, only the calculation of triton β decay [12,13], the related μ decay on ^{3}He and the deuteron [14], and proton-proton fusion [15] exhibits the required consistency, while the very recent calculation of the neutral-current response in ^{12}C employs phenomenological 3NFs and 2BCs [16].

The one-body operator $g_A \sum_{i=1}^{A} \sigma_i \tau_i^{\pm}$ induces Gamow-Teller transitions. Here, g_A is the axial-vector coupling, σ denotes the spin, and $\tau^{\pm}$ changes the isospin. Gamow-Teller strength functions [17,18] are also of particular interest because of their astrophysical relevance [19]. Charge-exchange measurements on ^{90}Zr and other medium-mass nuclei have suggested that the total strength for β decay is quenched by a factor of $q^2 \approx 0.88$–0.92 [20–23] when compared to the Ikeda sum rule [24]. Similarly, shell-model calculations [25,26] suggest that g_A needs to be quenched by a factor $q \approx 0.75$ to match data. It is not clear whether renormalizations (including 2BCs) of the employed Gamow-Teller operator, missing correlations in the nuclear wave functions, or model-space truncations are the cause of this quenching.

Recent calculations [27–29] show that chiral 2BCs yield an effective quenching of g_A. However, the Hamiltonians employed in these works are not consistent with the currents (and they contain no 3NFs) and/or the 2BCs are approximated by averaging the second nucleon over the Fermi sea of symmetric nuclear matter. The recent studies [30,31] of electroweak transitions in light nuclei employ 3NFs but lack 2BCs. This gives urgency for a calculation of weak decays that employs 3NFs and consistent 2BCs.

In this Letter, we address the quenching of g_A and employ 3NFs together with consistent 2BCs for the computation of β decays and the Ikeda sum rule. We study the β decays of ^{14}C and ^{22,24}O with interactions and currents from χEFT at next-to-next-to leading order (NNLO) for cutoffs $\Lambda_\chi = 450$, 500, 550 MeV. For the states of the daughter nuclei, we generalize a coupled-cluster technique and compute them as isospin-breaking excitations of the mother nuclei. We present predictions and spin assignments for the exotic isotopes ^{22,24}F and revisit the anomalously long half-life of ^{14}C [31–33].

Hamiltonian and model space.—The chiral nucleon-nucleon (NN) interactions are optimized to the proton-proton and the proton-neutron scattering data for laboratory

TABLE I. Pion-nucleon LECs c_i and partial-wave contact LECs (C, $\tilde{C}$) for the chiral NN interaction at NNLO using $\Lambda_\chi = 500$ MeV and the spectral-function regulator cutoff $\Lambda_{\rm SFR} = 700$ MeV [37]. The c_i, $\tilde{C}_i$, and C_i have units of GeV^{-1}, 10^4 GeV^{-2}, and 10^4 GeV^{-4}, respectively.

LEC	Value	LEC	Value	LEC	Value
c_1	−0.91940746	c_3	−3.88983848	c_4	4.307 367 47
$\tilde{C}^{pp}_{^1S_0}$	−0.15136364	$\tilde{C}^{np}_{^1S_0}$	−0.15215263	$\tilde{C}^{nn}_{^1S_0}$	−0.15180482
$C_{^1S_0}$	2.404 312 35	$C_{^3S_1}$	0.927 937 12	$\tilde{C}_{^3S_1}$	−0.15848125
$C_{^1P_1}$	0.414 829 08	$C_{^3P_0}$	1.265 789 78	$C_{^3P_1}$	−0.77998484
$C_{^3S_1-^3D_1}$	0.618 550 40	$C_{^3P_2}$	−0.67347042		

scattering energies below 125 MeV and to deuteron observables. The χ^2/datum varies between 1.33 for $\Lambda_\chi = 450$ MeV and 1.18 for $\Lambda_\chi = 550$ MeV. The χ^2 optimization employs the algorithm POUNDERS [34]. Table I shows the parameters of the NN interaction for the cutoff $\Lambda_\chi = 500$ MeV; the parameters for the other cutoffs are in the Supplemental Material [35]. The parameters displayed in Table I are close to those of the chiral interaction NNLO$_{\rm opt}$ [36], which were fit to phase shifts.

The 3NF is regularized with nonlocal cutoffs [38,39] (to mitigate the convergence problems documented by Hagen *et al.* [40] for local cutoffs). Following Gazit *et al.* [13], we optimize the two LECs (c_D and c_E) of the 3NF to the ground-state energies of $A = 3$ nuclei and the triton lifetime. Figure 1 shows the reduced transition matrix element $\langle E_1^A \rangle = \langle {}^3\mathrm{He}||E_1^A||{}^3\mathrm{H}\rangle$ as a function of c_D. Here, E_1^A is the $J = 1$ electric multipole of the weak axial-vector current at NNLO [13]. The leading-order (LO) contribution to E_1^A is proportional to the one-body Gamow-Teller operator $E_1^A|_{\rm LO} = i g_A (6\pi)^{-1/2} \sum_{i=1}^A \sigma_i \tau_i^\pm$. For the current, we use the empirical value $g_A = 1.2695(29)$ [41]. The 2BCs enter at NNLO and depend on the LECs c_D, c_3, c_4 of the chiral interaction [42,43]. The triton half-life yields an empirical value for $\langle E_1^A \rangle_{\rm emp}$, which constrains c_D and c_E. For the three different chiral cutoffs $\Lambda_\chi = 450, 500, 550$, the sets of

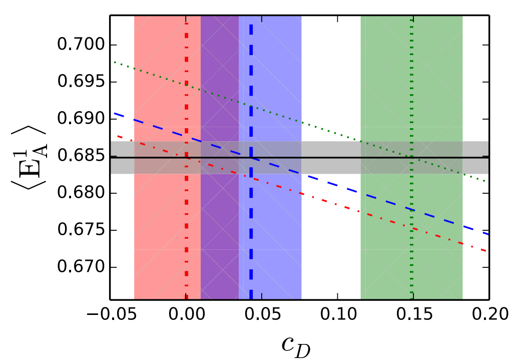

FIG. 1 (color online). The quantity related to the triton half-life $\langle E_1^A \rangle$ as a function c_D for chiral cutoffs $\Lambda_\chi = 450, 500, 550$ MeV (dash-dotted red, dashed blue, and dotted green lines, respectively) with corresponding error bands. The different lines were determined by a fit of c_D and c_E to $A = 3$ binding energies.

(c_D, c_E) that reproduce the triton half-life and the $A = 3$ binding energies are (0.0004, −0.4231), (0.0431, −0.5013), (0.1488, −0.7475), respectively. The vertical bands in Fig. 1 give the range of c_D that reproduces $\langle E_1^A \rangle_{\rm emp}$ within the experimental uncertainty.

We employ an $N = 12$ model space consisting of $N + 1$ oscillator shells with frequency $\hbar\Omega = 22$ MeV. The 3NFs use an energy cutoff of $E_{3\,\rm max} = N\hbar\Omega$; i.e., the sum of the excitation energies of three nucleons does not exceed $E_{3\,\rm max}$. We employ the intrinsic Hamiltonian $H = T - T_{\rm c.m.} + V_{NN} + V_{\rm 3NF}$ to mitigate any spurious center-of-mass excitations [44,45]. Here, T and $T_{\rm c.m.}$ are the kinetic energy and the kinetic energy of the center of mass, while V_{NN} and $V_{\rm 3NF}$ are the chiral NN interaction and 3NF, respectively.

We perform a Hartree-Fock (HF) calculation and compute the normal-ordered Hamiltonian H_N with respect to the reference state $|\mathrm{HF}\rangle$. We truncate H_N at the normal-ordered two-body level. This approximation is accurate in light- and medium-mass nuclei [46,47].

Formalism.—We compute the closed-subshell mother nuclei ^{14}C and ^{22,24}O with the coupled-cluster method [48–55]. The similarity-transformed Hamiltonian $\bar{H} \equiv e^{-T} H_N e^T$ employs the cluster amplitudes

$$T = \sum_{ia} t_i^a N_a^\dagger N_i + \frac{1}{4} \sum_{ijab} t_{ij}^{ab} N_a^\dagger N_b^\dagger N_j N_i \quad (1)$$

that create one-particle–one-hole ($1p$-$1h$) and two-particle–two-hole ($2p$-$2h$) excitations with amplitudes t_i^a and t_{ij}^{ab}, respectively. Here, i, j denote occupied orbitals of the HF reference while a, b denote orbitals of the valence space. The operators $N_q^\dagger$ and N_q create and annihilate a nucleon in orbital q, respectively. It is understood that the cluster amplitudes T do not change the number of protons and neutrons; i.e., they conserve the z component T_z of isospin. We note that $|\mathrm{HF}\rangle$ is the right ground state of the non-Hermitian Hamiltonian $\bar{H}$. Its left ground state is $\langle\Lambda| = \langle \mathrm{HF}|(1 + \Lambda)$, with Λ being a linear combination of $1p$-$1h$ and $2p$-$2h$ deexcitation operators [54,55].

The daughter nuclei ^{14}N and ^{22,24}F are computed via a novel generalization of the coupled-cluster equation-of-motion approach [56–58]. We view the states of the daughter nuclei as isospin-breaking excitations $|R\rangle \equiv R|\mathrm{HF}\rangle$ of the coupled-cluster ground state, with

$$R \equiv \sum_{ia} r_i^a p_a^\dagger n_i + \frac{1}{4} \sum_{ijab} r_{ij}^{ab} p_a^\dagger N_b^\dagger N_j n_i. \quad (2)$$

Here, $p_q^\dagger$ and p_q ($n_q^\dagger$ and n_q) create and annihilate a proton (neutron) in orbital q with amplitude r_i^a. The combination $N_q^\dagger N_s$ either involves neutrons $N_q^\dagger N_s = n_q^\dagger n_s$ or protons $N_q^\dagger N_s = p_q^\dagger p_s$ and goes with the excitation amplitude r_{ij}^{ab}. We note that R lowers the isospin component T_z of the HF reference by one unit and keeps the mass number unchanged.

The states of the daughter nucleus result from solving the eigenvalue problem $\bar{H}R_\alpha|\mathrm{HF}\rangle = \omega_\alpha R_\alpha|\mathrm{HF}\rangle$. Here, ω_α is the excitation energy with respect to the HF reference and R_α denotes a set of amplitudes $R_\alpha = (r_i^a(\alpha), r_{ij}^{ab}(\alpha))$. We also introduce the left-acting deexcitation operator

$$L \equiv \sum_{ia} l_a^i n_i^\dagger p_a + \frac{1}{4}\sum_{ijab} l_{ab}^{ij} n_i^\dagger N_j^\dagger N_b p_a \qquad (3)$$

and solve the left eigenvalue problem $\langle\mathrm{HF}|L_\beta\bar{H} = \omega_\beta\langle\mathrm{HF}|L_\beta$. Here, l_a^i and l_{ab}^{ij} are the corresponding $1p$-$1h$ and $2p$-$2h$ deexcitation amplitudes. The left and right eigenvectors are biorthogonal, i.e., $\langle\mathrm{HF}|L_\alpha R_\beta|\mathrm{HF}\rangle = \sum_{ia} l_a^i(\alpha) r_i^a(\beta) + \frac{1}{4}\sum_{ijab} l_{ab}^{ij}(\alpha) r_{ij}^{ab}(\beta) = \delta_{\alpha\beta}$.

The operators R and L in Eqs. (2) and (3) excite states in the daughter nucleus that results from β^- decay. If instead we were interested in β^+ decay, we would employ $R^\dagger$ and $L^\dagger$ and solve the corresponding eigenvalue problems. Our approach allows us to compute excited states in the daughter nucleus that are dominated by isospin-breaking $1p$-$1h$ excitations of the closed-shell reference $|\mathrm{HF}\rangle$ (with $2p$-$2h$ excitations being smaller corrections).

Results.—The spectra for ^{14}N and ^{22,24}F are shown in Fig. 2 for $\Lambda_\chi = 500$ MeV and compared to data. The sensitivity of our results on the chiral cutoff Λ_χ is shown as bands for selected states. The odd-odd daughter nuclei ^{14}N and ^{22,24}F exhibit a higher level density than their mother nuclei. Overall, 3NFs increase the level densities slightly and yield a slightly improved comparison to experiment. For ^{22,24}F, we make several predictions and spin assignments. In these isotopes, our spectra also compare well to shell-model calculations by Brown and Richter [59]. Low-lying excitation energies changed by less than 5% when going to $E_{3\,\max} = 14\hbar\Omega$, and 15% is an error estimate including the error from truncating at the coupled-cluster $2p$-$2h$ level.

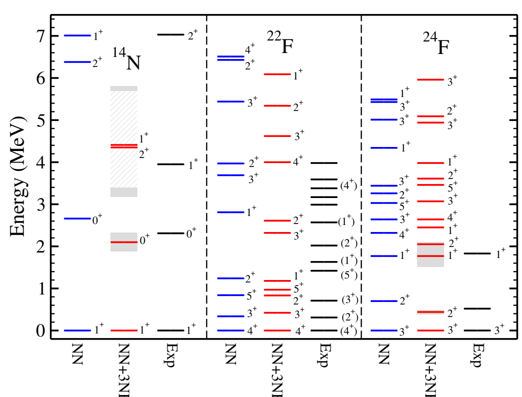

FIG. 2 (color online). Spectra of the odd-odd daughter nuclei ^{14}N and ^{22,24}F resulting from the NN interaction with chiral cutoff $\Lambda_\chi = 500$ MeV (blue lines) and the NN interaction and 3NF at NNLO with chiral cutoff $\Lambda_\chi = 500$ MeV (red lines), compared to experiment (black lines). Bands from variation of the chiral cutoff $\Lambda_\chi = 450$–550 MeV are shown for the $0^+, 2^+, 1^+$ and the $2^+, 1^+$ excited states in ^{14}N and ^{24}F, respectively. The band with diagonal gray lines in ^{14}N is for the 1^+ excited state. Parentheses indicate tentative spin-parity assignments.

For a better assessment of systematic uncertainties, we compared the results at LO, NLO, and NNLO for $\Lambda_\chi = 500$ MeV. For the ground-state energy of ^{14}C, we find −60.5, −93.2, and −74.4 MeV, respectively, hinting at a slow convergence with respect to the chiral power counting and a significant underbinding with respect to the experimental value of −105.3 MeV. Similar results are obtained for ^{22,24}O. The convergence is faster for the excited states. The excited $J^\pi = 0^+$ ($J^\pi = 1^+$) [$J^\pi = 2^+$] state in ^{14}N is at 2.1, 2.8, 2.1 MeV (1.7, 5.6, 4.4 MeV) [0.7, 4.9, 4.4 MeV] in LO, NLO, NNLO, respectively. We also note that the ground-state energies of the daughter nuclei ^{14}N, ^{22,24}F are 0.54, −2.62, and −6.55 MeV with respect to their corresponding mother nuclei, in fair agreement with experiment. Thus, the systematic uncertainty due to the Hamiltonian is significant for ground states but less of a concern for the excited states discussed in this Letter. The underbinding of the present Hamiltonian suggests that the role of 3NFs and/or higher-order EFT corrections might be more complicated than proposed by Ekström *et al.* [36].

Within the coupled-cluster framework, we compute the total strengths

$$S_+ = \langle\Lambda|\overline{\hat{O}_{\mathrm{GT}}}\,\overline{\hat{O}_{\mathrm{GT}}^\dagger}|\mathrm{HF}\rangle, \qquad S_- = \langle\Lambda|\overline{\hat{O}_{\mathrm{GT}}^\dagger}\,\overline{\hat{O}_{\mathrm{GT}}}|\mathrm{HF}\rangle$$

for $\beta^\pm$ decays. Here, $\overline{\hat{O}_{\mathrm{GT}}}$ is the similarity-transformed Gamow-Teller operator

$$\hat{O}_{\mathrm{GT}} \equiv \hat{O}_{\mathrm{GT}}^{(1)} + \hat{O}_{\mathrm{GT}}^{(2)} \equiv g_A^{-1}\sqrt{3\pi}E_1^A. \qquad (4)$$

The one-body operator is $\hat{O}_{\mathrm{GT}}^{(1)} = g_A^{-1}\sqrt{3\pi}E_1^A|_{\mathrm{LO}}$, and the two-body operator $\hat{O}_{\mathrm{GT}}^{(2)}$ is from the 2BC at NNLO, with a local regulator and with the same cutoff as the interaction [42,43].

The Ikeda sum rule is $S_- - S_+ = 3(N-Z)$ for $\hat{O}_{\mathrm{GT}} = \hat{O}_{\mathrm{GT}}^{(1)}$. This identity served as a check of our calculations. Our interest, of course, is in the contribution of the 2BC operator $\hat{O}_{\mathrm{GT}}^{(2)}$ to the total β decay strengths $S_\pm$. We considered two approximations of this two-body operator. In the normal-ordered one-body approximation (NO1B), the second fermion of the 2BC is summed over the occupied states of the HF reference. In the second approximation, we add the two-body operator $\overline{\hat{O}_{\mathrm{GT}}^{(2)}} \approx \hat{O}_{\mathrm{GT}}^{(2)}$ to the NO1B contribution. This is the LO coupled-cluster contribution of $\overline{\hat{O}_{\mathrm{GT}}^{(2)}}$, and it is a smaller correction to the NO1B contribution for the nuclei we study.

Figure 3 shows the quenching factor $q^2 = (S_- - S_+)/[3(N-Z)]$ for ^{14}C and ^{22,24}O. For the cutoff $\Lambda_\chi = 500$ MeV, we vary c_D between −0.9 and 0.9 and fix c_E such that the binding energies of the $A=3$ nuclei are

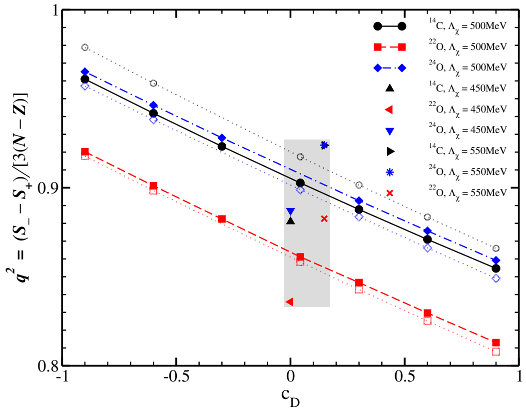

FIG. 3 (color online). The quenching factor q^2 for ^{14}C (solid black line), ^{22}O (dashed red line), and ^{24}O (dash-dotted blue line) for different c_D values. The calculations used NN and 3NF with consistent 2BCs. The gray area marks the region of c_D that yields the triton half-life and shows the cutoff dependence. The dotted lines show the NO1B results.

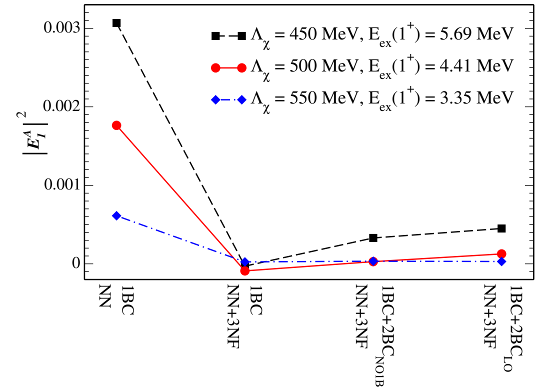

FIG. 4 (color online). The squared transition matrix element for β^- decay of ^{14}C from increasingly sophisticated calculations (from left to right). NN, 1BC: NN interactions and one-body currents (1BCs) only; $NN+3$NF, 1BC: addition of 3NF; $NN+3$NF, $1\mathrm{BC}+2\mathrm{BC}_{\mathrm{NO1B}}$: addition of 2BC in the NO1B approximation; and $NN+3$NF, $1\mathrm{BC}+2\mathrm{BC}_{\mathrm{LO}}$: addition of leading-order 2BC.

reproduced. The ground-state energies and excited states in ^{14}C and ^{22,24}F are insensitive to this variation. Thus, the dependence of $(S_- - S_+)/[3(N-Z)]$ on c_D is due to 2BCs. The NO1B approximation (shown as dotted lines) yields a major part of the quenching. The sensitivity of our results to the chiral cutoffs ($\Lambda_\chi = 450$, 500, 550 MeV) is shown as the gray band for values of c_D and c_E that reproduce the triton half-life. The quenching factor depends on the nucleus, with $q^2 \approx 0.84$–0.92 due to 2BCs for the studied nuclei, consistent with Ref. [28]. We recall that $q^2 \approx 0.88$–0.92, extracted from experiments on ^{90}Zr [21–23], are within our error band. We also computed the low-lying strengths for β^- decay and found that only 70%–80% of the total strength $S_\pm$ is exhausted below 10 MeV of excitation energy.

Let us finally turn to the β^- decay of ^{14}C. The long half-life of this decay, about 5700a, is used in carbon dating of organic material. This half-life is anomalously long in the sense that it exceeds the half-lives of neighboring β unstable nuclei by many orders of magnitude. Recently, several studies attributed the long half-life of ^{14}C to 3NFs [31–33], while the experiment points to a complicated strength function [60]. What do 2BCs contribute to this picture? To address this question, we compute the matrix element $\langle E_1^A \rangle \equiv \langle ^{14}\mathrm{N}|E_1^A|^{14}\mathrm{C}\rangle$ that governs the β^- decay of ^{14}C to the ground state of ^{14}N, with c_D and c_E from the triton lifetime. Figure 4 shows the various contributions to the matrix element. In agreement with Maris *et al.* [31] and Holt *et al.* [33], 3NFs reduce the matrix element significantly in size, and our result is similar in magnitude to that reported by Maris *et al.* [31]. However, 2BCs counter this reduction to some extent, with the NO1B approximation and the LO approximation both giving significant contributions. Our results for $\langle E_1^A \rangle$ from 2BCs and 3NFs are between 5×10^{-3} and 2×10^{-2}. This is more than an order of magnitude larger than the empirical value $\langle E_1^A \rangle_{\mathrm{emp}} \approx 6\times10^{-4}$ extracted from the 5700a half-life of ^{14}C. In β^- decay of ^{14}C, 2BCs increase the strength of the transition to the ^{14}N ground state, while they yield an overall quenching (of the sum rule) when all transitions are considered.

We also find that the matrix element $\langle E_1^A \rangle$ depends on the energy of the first excited 1^+ state in ^{14}N. For the three different cutoffs $\Lambda_\chi = 450$, 500, 550 MeV, this excited 1^+ state is at 5.69, 4.41, 3.35 MeV, respectively (compared to 3.95 MeV from experiment). As the value of $\langle E_1^A \rangle$ decreases strongly with decreasing excitation energy, a correct description of this state is important for the half-life in ^{14}C.

Summary.—We studied β^- decays of ^{14}C and ^{22,24}O. Because of 2BCs, we found a quenching factor $q^2 \approx 0.84$–0.92 from the difference in total β decay strengths $S_- - S_+$ when compared to the Ikeda sum rule value $3(N-Z)$. To carry out this study, we optimized interactions from χEFT at NNLO to scattering observables for chiral cutoffs $\Lambda_\chi = 450$, 500, 550 MeV. We developed a novel coupled-cluster technique for the computation of spectra in the daughter nuclei and made several predictions and spin assignments in the exotic neutron-rich isotopes of fluorine. We find that 3NFs increase the level density in the daughter nuclei and thereby improve the comparison to data. The anomalously long half-life for the β^- decay of ^{14}C depends in a complicated way on 3NFs and 2BCs. While the former increase the theoretical half-life, the latter somewhat counter this effect. Taken together, the inclusion of 3NFs and 2BCs yields an increase in the computed half-life.

We thank D. J. Dean, J. Engel, Y. Fujita, K. Hebeler, M. Hjorth-Jensen, M. Sasano, T. Uesaka, and A. Signoracci for useful discussions. We also thank E. Epelbaum for providing us with nonlocal 3NF matrix elements. This work was supported by the Office of Nuclear Physics, U.S. Department of Energy (Oak Ridge National Laboratory), under DE-FG02-96ER40963 (University of Tennessee), DE-SC0008499 (NUCLEI SciDAC Collaboration), and the Field Work Proposal ERKBP57 at Oak Ridge National Laboratory; by the National Research Council and by the Nuclear Science and Engineering Research Council of Canada. The work of D. G. is supported by a German-Israeli Research Award Funded by the Federal German Ministry for Education and Research (BMBF) and Administered by Minerva. Computer time was provided by the Innovative and Novel Computational Impact on Theory and Experiment (INCITE) Program. This research used resources of the Oak Ridge Leadership Computing Facility located in the Oak Ridge National Laboratory, which is supported by the Office of Science of the Department of Energy under Contract No. DE-AC05-00OR22725, and used computational resources of the National Center for Computational Sciences, the National Institute for Computational Sciences, and the Notur Project in Norway.

[1] F. T. Avignone, S. R. Elliott, and J. Engel, Rev. Mod. Phys. **80**, 481 (2008).

[2] J. A. Winger, S. V. Ilyushkin, K. P. Rykaczewski, C. J. Gross, J. C. Batchelder, C. Goodin, R. Grzywacz, J. H. Hamilton, A. Korgul, W. Królas *et al.*, Phys. Rev. Lett. **102**, 142502 (2009).

[3] K. Miernik, K. P. Rykaczewski, C. J. Gross, R. Grzywacz, M. Madurga, D. Miller, J. C. Batchelder, I. N. Borzov, N. T. Brewer, C. Jost *et al.*, Phys. Rev. Lett. **111**, 132502 (2013).

[4] R. Schiavilla and R. B. Wiringa, Phys. Rev. C **65**, 054302 (2002).

[5] J. Fujita and H. Miyazawa, Prog. Theor. Phys. **17**, 360 (1957).

[6] U. van Kolck, Phys. Rev. C **49**, 2932 (1994).

[7] E. Epelbaum, H.-W. Hammer, and U.-G. Meißner, Rev. Mod. Phys. **81**, 1773 (2009).

[8] S. Kölling, E. Epelbaum, H. Krebs, and U. G. Meißner, Phys. Rev. C **80**, 045502 (2009).

[9] H. Grießhammer, J. McGovern, D. Phillips, and G. Feldman, Prog. Part. Nucl. Phys. **67**, 841 (2012).

[10] S. Pastore, S. C. Pieper, R. Schiavilla, and R. B. Wiringa, Phys. Rev. C **87**, 035503 (2013).

[11] S. Bacca and S. Pastore, J. Phys. G **41**, 123002 (2014).

[12] A. Gårdestig and D. R. Phillips, Phys. Rev. Lett. **96**, 232301 (2006).

[13] D. Gazit, S. Quaglioni, and P. Navrátil, Phys. Rev. Lett. **103**, 102502 (2009).

[14] L. E. Marcucci, A. Kievsky, S. Rosati, R. Schiavilla, and M. Viviani, Phys. Rev. Lett. **108**, 052502 (2012).

[15] L. E. Marcucci, R. Schiavilla, and M. Viviani, Phys. Rev. Lett. **110**, 192503 (2013).

[16] A. Lovato, S. Gandolfi, J. Carlson, S. C. Pieper, and R. Schiavilla, Phys. Rev. Lett. **112**, 182502 (2014).

[17] R. G. T. Zegers, T. Adachi, H. Akimune, S. M. Austin, A. M. van den Berg, B. A. Brown, Y. Fujita, M. Fujiwara, S. Galès, C. J. Guess *et al.*, Phys. Rev. Lett. **99**, 202501 (2007).

[18] Y. Fujita, H. Fujita, T. Adachi, C. L. Bai, A. Algora, G. P. A. Berg, P. von Brentano, G. Colò, M. Csatlós, J. M. Deaven *et al.*, Phys. Rev. Lett. **112**, 112502 (2014).

[19] K. Langanke, G. Martínez-Pinedo, J. M. Sampaio, D. J. Dean, W. R. Hix, O. E. B. Messer, A. Mezzacappa, M. Liebendörfer, H.-T. Janka, and M. Rampp, Phys. Rev. Lett. **90**, 241102 (2003).

[20] H. Sakai, T. Wakasa, H. Okamura, T. Nonaka, T. Ohnishi, K. Yako, K. Sekiguchi, S. Fujita, Y. Satou, H. Otsu *et al.*, Nucl. Phys. **A649**, 251 (1999).

[21] K. Yako, H. Sakai, M. Greenfield, K. Hatanaka, M. Hatano, J. Kamiya, H. Kato, Y. Kitamura, Y. Maeda, C. Morris *et al.*, Phys. Lett. B **615**, 193 (2005).

[22] M. Ichimura, H. Sakai, and T. Wakasa, Prog. Part. Nucl. Phys. **56**, 446 (2006).

[23] M. Sasano, H. Sakai, K. Yako, T. Wakasa, S. Asaji, K. Fujita, Y. Fujita, M. B. Greenfield, Y. Hagihara, K. Hatanaka *et al.*, Phys. Rev. C **79**, 024602 (2009).

[24] K. Ikeda, S. Fujii, and J. Fujita, Phys. Lett. **3**, 271 (1963).

[25] W.-T. Chou, E. K. Warburton, and B. A. Brown, Phys. Rev. C **47**, 163 (1993).

[26] G. Martínez-Pinedo, A. Poves, E. Caurier, and A. P. Zuker, Phys. Rev. C **53**, R2602 (1996).

[27] S. Vaintraub, N. Barnea, and D. Gazit, Phys. Rev. C **79**, 065501 (2009).

[28] J. Menéndez, D. Gazit, and A. Schwenk, Phys. Rev. Lett. **107**, 062501 (2011).

[29] J. Engel, F. Simkovic, and P. Vogel, Phys. Rev. C **89**, 064308 (2014).

[30] M. Pervin, S. C. Pieper, and R. B. Wiringa, Phys. Rev. C **76**, 064319 (2007).

[31] P. Maris, J. P. Vary, P. Navrátil, W. E. Ormand, H. Nam, and D. J. Dean, Phys. Rev. Lett. **106**, 202502 (2011).

[32] J. W. Holt, G. E. Brown, T. T. S. Kuo, J. D. Holt, and R. Machleidt, Phys. Rev. Lett. **100**, 062501 (2008).

[33] J. W. Holt, N. Kaiser, and W. Weise, Phys. Rev. C **79**, 054331 (2009).

[34] M. Kortelainen, T. Lesinski, J. Moré, W. Nazarewicz, J. Sarich, N. Schunck, M. V. Stoitsov, and S. Wild, Phys. Rev. C **82**, 024313 (2010).

[35] See Supplemental Material at http://link.aps.org/supplemental/10.1103/PhysRevLett.113.262504 for the low-energy coupling constants of the chiral interactions with chiral cutoffs 450 and 500 MeV.

[36] A. Ekström, G. Baardsen, C. Forssén, G. Hagen, M. Hjorth-Jensen, G. R. Jansen, R. Machleidt, W. Nazarewicz, T. Papenbrock, J. Sarich *et al.*, Phys. Rev. Lett. **110**, 192502 (2013).

[37] E. Epelbaum, W. Glöckle, and U.-G. Meißner, Eur. Phys. J. A **19**, 401 (2004).

[38] E. Epelbaum, A. Nogga, W. Glöckle, H. Kamada, U.-G. Meißner, and H. Witała, Phys. Rev. C **66**, 064001 (2002).

[39] K. Hebeler, Phys. Rev. C **85**, 021002 (2012).

[40] G. Hagen, T. Papenbrock, A. Ekström, K. A. Wendt, G. Baardsen, S. Gandolfi, M. Hjorth-Jensen, and C. J. Horowitz, Phys. Rev. C **89**, 014319 (2014).

[41] C. Amsler, M. Doser, M. Antonelli, D. Asner, K. Babu, H. Baer, H. Band, R. Barnett, E. Bergren, J. Beringer *et al.*, Phys. Lett. B **667**, 1 (2008).

[42] T.-S. Park, L. E. Marcucci, R. Schiavilla, M. Viviani, A. Kievsky, S. Rosati, K. Kubodera, D.-P. Min, and M. Rho, Phys. Rev. C **67**, 055206 (2003).
[43] D. Gazit, Phys. Lett. B **666**, 472 (2008).
[44] G. Hagen, T. Papenbrock, and D. J. Dean, Phys. Rev. Lett. **103**, 062503 (2009).
[45] G. R. Jansen, Phys. Rev. C **88**, 024305 (2013).
[46] G. Hagen, T. Papenbrock, D. J. Dean, A. Schwenk, A. Nogga, M. Włoch, and P. Piecuch, Phys. Rev. C **76**, 034302 (2007).
[47] R. Roth, S. Binder, K. Vobig, A. Calci, J. Langhammer, and P. Navrátil, Phys. Rev. Lett. **109**, 052501 (2012).
[48] F. Coester, Nucl. Phys. **7**, 421 (1958).
[49] F. Coester and H. Kümmel, Nucl. Phys. **17**, 477 (1960).
[50] J. Čížek, J. Chem. Phys. **45**, 4256 (1966).
[51] J. Čížek, *On the Use of the Cluster Expansion and the Technique of Diagrams in Calculations of Correlation Effects in Atoms and Molecules* (Wiley, New York, 2007), p. 35.
[52] H. Kümmel, K. H. Lührmann, and J. G. Zabolitzky, Phys. Rep. **36**, 1 (1978).
[53] D. J. Dean and M. Hjorth-Jensen, Phys. Rev. C **69**, 054320 (2004).
[54] R. J. Bartlett and M. Musiał, Rev. Mod. Phys. **79**, 291 (2007).
[55] G. Hagen, T. Papenbrock, M. Hjorth-Jensen, and D. J. Dean, Rep. Prog. Phys. **77**, 096302 (2014).
[56] J. F. Stanton and R. J. Bartlett, J. Chem. Phys. **98**, 7029 (1993).
[57] J. R. Gour, P. Piecuch, M. Hjorth-Jensen, M. Włoch, and D. J. Dean, Phys. Rev. C **74**, 024310 (2006).
[58] G. R. Jansen, M. Hjorth-Jensen, G. Hagen, and T. Papenbrock, Phys. Rev. C **83**, 054306 (2011).
[59] B. A. Brown and W. A. Richter, Phys. Rev. C **74**, 034315 (2006).
[60] A. Negret, T. Adachi, B. R. Barrett, C. Bäumer, A. M. van den Berg, G. P. A. Berg, P. von Brentano, D. Frekers, D. De Frenne, H. Fujita *et al.*, Phys. Rev. Lett. **97**, 062502 (2006).